Organised by the Institution of Engineering and Technology Measurement, Sensors, Instrumentation & NDT and Microsystems and Nanotechnology Networks

Suspension-Compatible Elastomer-Glass Micropumps Employing a Linear Topology

M C Tracey
STRI University of Hertfordshire, UK

Printed and published by the Institution of Engineering and Technology, Michael Faraday House, Six Hills Way, Stevenage, Herts SG1 2AY, UK

About the Speaker

Dr. Mark Tracey is Reader in Microfluidics at the University of Hertfordshire, Hatfield. Whilst an electronics engineer by training, Mark's career has been somewhat multidisciplinary. He commenced researching microfluidics 15 years ago with his PhD concerning blood cell mechanical measurements with microfluidics. His research group now conducts both academic and commercial research. Other than micropumps, current academic work involves human stem cell culture, particle sorting, vapour sensing and micromixing. Commercial activities typically concern the development of turn-key instrumentation incorporating microfluidics.

SUSPENSION-COMPATIBLE ELASTOMER-GLASS MICROPUMPS EMPLOYING A LINEAR TOPOLOGY

M.C.Tracey*, I.D.Johnston, J.B.Davis, C.K.L.Tan

*STRI, University of Hertfordshire, Hatfield, AL10 9AB

Keywords: suspension-compatible, micropump, elastomer, soft-lithography.

Abstract

We report a simple, high pumping performance, micropump comprising a narrow flow channel with integral flow control structures operated by a single actuator element. Unusually, it does not have a distinct pump chamber. This micropump is termed a 'Linear MTP' (LMTP) as it exploits the microthrottling principle and single actuator operation of MTP devices we have previously reported. Uncharacteristically for a micropump and in common with all MTPs, the device is compatible with solid phase suspensions.

The flow-channel-like, linear pump minimises the development of recirculatory flows that are typically associated with circular pump chambers and in part, determine the frequency response and hence maximum pumping rates of many micropumps. The actuation of linear pumps by flexing, bimorphic, discoidal actuators is possible by virtue of an elastomeric substrate which allows actuator flexure over solid substrate regions whilst to some degree constructively coupling the forces in those regions into active regions.

We have modelled, fabricated and evaluated an LMTP that yields a maximum pumping rate of circa 1.15 ml min^{-1} and a back pressure of 39 kPa at a drive frequency of 1.8 kHz. Images of 5μm polystyrene beads flowing within the LMTP confirm minimal recirculatory flow consistent with the LMTP's increased operating frequencies compared to previous circular pump chamber MTPs.

1 Introduction

We have previously reported [2-4] the mechanism of 'micro-throttling': the use of variable cross-section flow-constrictions to regulate fluid flow. Microthrottles are very applicable to micropumps that we term Micro Throttle Pumps (MTPs). Microthrottles exploit the use, in part or wholly, of elastomeric substrates. The fact that microthrottles do not actually close, allied to their construction from compliant materials, makes them highly suited to the pumping of solid phase suspensions such as polystyrene microbeads, as we have previously reported [3]. Unlike conventional seal valves, microthrottles only display partial closure, yet when incorporated in MTPs their resulting, relatively modest, closed-to-open fluid flow resistance ratios (throttling ratios) result in pumping efficiencies close to those of pumps with classic, fully-closing valves. However, it is to be noted that they do differ by not displaying a 'normally-closed' valve-like behaviour when not energised.

We originally reported [2] an MTP with two microthrottles and a pump chamber as three, distinct, PZT-actuated, poly(dimethylsiloxane) (PDMS)-glass microfluidic components. Whilst demonstrating the MTP principle, the first MTP had a modest pumping rate due to the lower throttling ratios then achievable with a deep-narrow, 'slot', throttle design and frequency limitations imposed by fluidic interconnections between the constituent components. Subsequently [3], we reported a technique that allowed all three elements to be integrated within a single substrate and actuated by a single PZT actuator by virtue of a mode of bi-directional flexure within the composite structure. Whilst yielding a desirably compact structure which demonstrated the pumping of polystyrene beads, this technique reduced the pumping rate by a factor of 2.3 times to 132 μl min^{-1}, however back-pressure remained essentially unchanged at 6.0 kPa due to the unchanged throttle design. Subsequently, we reported an MTP that retained the single PZT actuator configuration but incorporated a new, more efficient, 'double-depth' throttle [4]. The superior throttling ratio of a double-depth throttle, in conjunction with 'displacement amplification' (to be discussed later) yielded a throttling ratio of circa 8:1 with a consequent increase in pump rate to 630 μl min^{-1} along with a five-fold increase in back-pressure to 30 kPa

2 Integration of pump functions within an elastomeric substrate.

At the heart of a classical piezoelectrically actuated, rigid substrate micropump is a circular pump chamber extending beyond the perimeter of the piezoelectric actuator in order to allow, to a first order, unrestricted flexure of the pump chamber diaphragm to which the actuator is bonded [5, 6]. As we have previously discussed, elastomeric substrates allow substrate material to substantially impinge below the footprint of the actuator provided that other design constraints are

considered [3, 4]. Accordingly it is not, per se, necessary for the pump chamber to match either the size or shape of the piezoelectric actuator. In the work reported here this allows the use of a linear pump chamber: which would not be feasible in a rigid substrate pump.

2.1 Linear MTPs

Our earlier single actuator MTPs consisted of 400µm wide inlet and outlet channels incorporating two 1mm wide, carefully located, (to benefit from bidirectional flexure) microthrottles. A 3mm diameter pump chamber was positioned between the microthrottles. In the LMTP the pump chamber has now evolved into a distributed component of the interconnecting channel between the two throttles. This design allows higher frequency operation by minimising frequency dependent, recirculatory effects within the pump chamber such as those described by Andersson et al [1] which result in pumping losses.

Thus far, our reported work has concentrated on increasing pumping efficiency via refinement of microthrottling; the pumping chamber itself has remained relatively unchanged. Whilst the LMTP, without an explicit pump chamber, represents a significant variation in MTP design we retained previous optimisations concerning *single-actuator operation, bidirectional-deflection* and *displacement-amplification.*

3 Design and Modelling.

In order to in order to illustrate our discussion of the principles of the LMTP within the space constraints of this paper, we have deliberately brought forward to this point in the paper SEM images of the microcast LMTP structures, a composite device cross section and an image of a complete device.

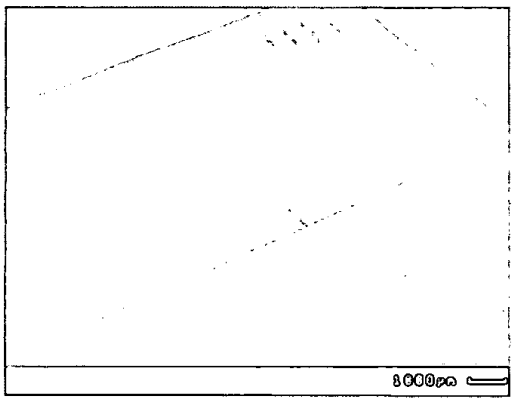

Figure 1: SEM of LMTP PDMS substrate.

Figure 1 shows the basic PDMS structure consisting of the characteristic 'flow-channel' running the length of the device between two circular areas that will subsequently be punched-through to form through-vias. Careful observation will show the two microthrottles, it is to be noted that they are deliberately asymmetric.

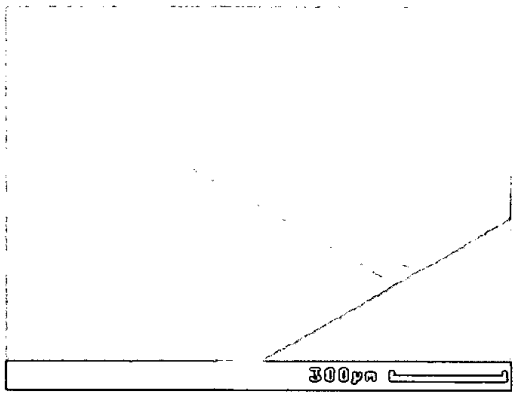

Figure 2: SEM of double depth microthrottle.

Reference to figure 4 clarifies that this allows the two microthrottles to be placed at points undergoing antiphase deflection hence providing the basic mechanism of flow-sequencing. Figure 2 shows a microthrottle in detail, the throttle is displaced downwards in the substrate by 15 µm by means of double-depth molding. The resulting gap between the top of the throttle and the subsequently bonded top-plate defined the microthrottle operating gap which is modulated by a combination of direct deflection of the upper glass via piezoelectric deflection and indirect, opposing deflection of microthrottle PDMS by means of 'displacement amplification'[4].

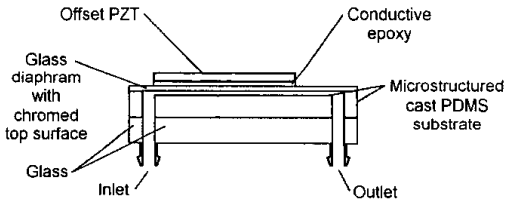

Figure 3. Simplified sectional schematic of an LMTP.

Figure 3 illustrates an assembled LMTP, the offset positioning of the piezoelectric actuator should be noted, this is a deliberate strategy as illustrated in figure 4 whereby it is possible to extend the area of reverse flexure within the structure by offset positioning. This extended area facilitates the positioning of microfluid structures within the underlying substrate area.

ANSYS V9.0 (ANSYS Inc.) was employed to further develop our earlier FEM models in order to validate that a linear pump design employing the displacement amplification effect [4] would provide a worthwhile displaced volume per pumping stroke under conditions of low-frequency, zero back-pressure operation. Whilst an account of FEM modelling is beyond the

space constraints of this paper, certain aspects of behaviour can be introduced and illustrated.

Materials properties, overall external dimensions and layer thicknesses, were unchanged from those we have employed previously [4]. Specifically we modelled a PZT bimorph disc 12.7 mm in diameter and of 410 μm thickness bonded to a borosilicate microscope slide cover slip 18 mm square and 110 μm thick with this composite, in turn, bonded to a layer of PDMS (Dow Corning Sylgard 184) 18 mm square and 1.5 mm thick. The elastic moduli used were 52 GPa, 73 GPa and 1 MPa respectively for the PZT actuator disc, glass and PDMS; the corresponding values of Poisson's Ratio were 0.31, 0.30 and 0.4999.

Our previous laser interferometric measurements [3] determined that piezoelectric actuator/glass/PDMS/glass structures with this general form, materials properties and dimensions display a linear displacement/voltage relationship, normal to the central axis of the piezoelectric actuator, of approximately 0.018 μm V^{-1}. It should be noted that the piezoelectric actuators employed (Piezo Systems, MA, USA, T216-A4NO-273X) are intrinsic bimorphs displaying symmetric, bidirectional deflection when subject to equal magnitude positive and negative potentials. Modelling determined the deformations generated by the actuator's maximum working voltage of ± 180 V.

The FEM modelling generated data of fig. 4 illustrates the concurrent, bidirectional flexure of the upper surface of the LMTP about its resting state which facilitates the opposing operation of the two microthrottles and hence pump sequencing.

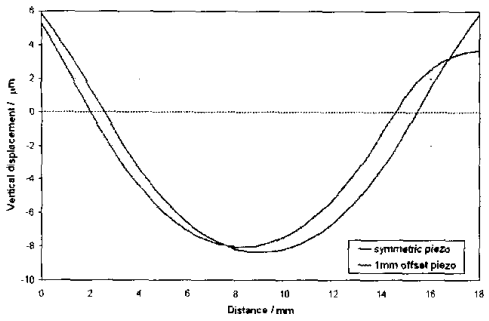

Figure 4: sectional profile of LMTP's upper surface deflection for cases of a symmetrically positioned actuator and an offset one.

Figure 4 also displays the deliberate, predicted 'plateau' of reversed flexure to the right side, below which one of the microthrottles is aligned. This is clearly confirmed in the Laser-vibrometric (Polytec PSV400-series scanning laser vibrometer, Lambda Photometrics, Harpenden, UK) experimental results of figure 5. Laser Vibrometry is a very valuable, non-contact, displacement imaging technique that allows quasi real-time imaging of a system under dynamic conditions.

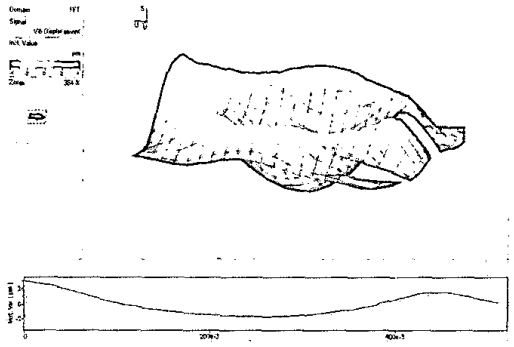

Figure 5: Laser-vibrometric image from a quasi-real-time sequence of a general, flexing, MTP structure. Left-right orientation agrees with figure 4. Right hand cut-outs are deliberate and coincide with bond wires.

Figure 6, whilst a generic illustration, serves to clarify the principle of 'displacement amplification'. The figure shows a bound surface (for instance the bonded glass top-plate) with a central aperture though which the free surface of the elastomer (PDMS) can expand. The other surfaces of the elastomer are considered to be effectively bound. As is intuitively obvious, a small downwards deflection of the bound surface results in much larger upwards displacement of the smaller free surface as we have discussed in detail elsewhere [4]. Of particular importance is the antiphase nature of the deflection. In order to benefit from this effect it is necessary to carefully design internal structures so as to concentrate such deflection as it the case in the LMTP's microthrottles whereby the PDMS structure is designed to move constructively with respect to the top cover in order to enhance throttling range.

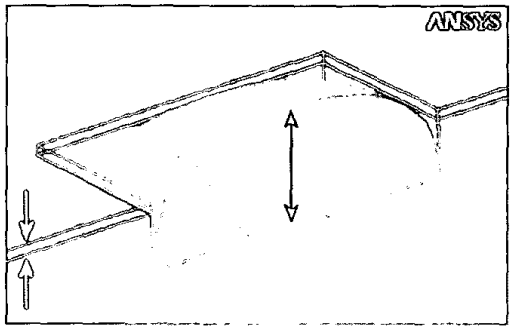

Figure 6: Generic illustration of displacement amplification in an elastomeric substrate. Upper, bound surface, save for aperture, is rigid.

4 Fabrication and assembly

The devices were fabricated and assembled in the general manner that we have previously described [3, 4], however, for

clarity we will summarise this process again. We commence by microfabricating molds from SU8 (Microchemcorp, MA, USA) structural photoresist. SU8 is well suited to rapid prototyping, allowing the formation of deep microstructures without recourse to expensive processing techniques. Photolithography was performed with 4040dpi, laser plotted, film photomasks. Double depth molds were fabricated on 3 inch Si wafers from two layers of SU-8 (SU-8 2025 and 2050) with general process parameters as per the manufacturer's recommendations. The double-depth process sequence ensures a planar surface for coating the second SU8 layer by exposing, but not subsequently developing, the first layer prior to spinning the thicker second layer over it. By this means, developed, physical, features in the first layer do not interfere with our ability to conformally spin on the second layer of photoresist. Accordingly, a 'thin' 15 μm thick SU-8 layer (that will form the throttle gap in the mold) was spun, pre-exposure baked, and subsequently patterned with a contact aligner. The wafer was then post-exposure baked. The thick 100 μm layer was then spun over, so as to bury, the thin layer and the composite was pre-exposure baked again. The second photomask was then aligned to the patterned first layer and exposed. It is to be noted that the second layer's exposed areas are a geometric subset of the first. The composite wafer was then post-exposure baked and developed to produce the mold.

The resulting mold was then incorporated as the base of a casting frame machined from 1.5 mm thick PMMA with a PMMA cover plate resulting in a 1.5 mm deep casting chamber. Dow Corning Sylgard 184 PDMS was prepared as a standard formulation according to manufacturer's instructions with particular care to both thoroughly mix the precursors and degas the resulting mix under vacuum before use. Once filled, the jig was placed in a fan-oven at 65 °C for 4 hours. the PDMS sheet cut into separate 18 mm square 'chips'. Through-vias were then punched through the chips with a sharpened 0.5 mm, thin-wall, stainless steel tube.

We then prepared the lower support glass and the thin upper plate. The support glass was 1.2 mm thick soda-lime glass microscope slide cut to 18 mm × 20 mm and diamond drilled to match the design's two connection vias. The upper glass was an 18 mm square, 110 μm thick, borosilicate coverglass (Menzel-Gläser, Braunschweig, Germany) whose upper face was coated with circa 250 nm of chrome by evaporation to provide for electrical connection to the lower PZT electrode. The appropriate faces of the PDMS, coverglass and microscope slide were then UV-Ozone treated to facilitate subsequent hydroxyl bonding, assembled and then baked at 90 °C for 2 hours to complete the PDMS-glass bonding. Figure 3 shows a schematic of the assembled device. The 12.7 mm diameter, piezoelectric actuator disc was then appropriately aligned and bonded to the top of the coverglass with conductive epoxy adhesive (Chemtronics, GA, USA) and fine connecting wires were attached. An assembled LMTP can be seen in figure 7.

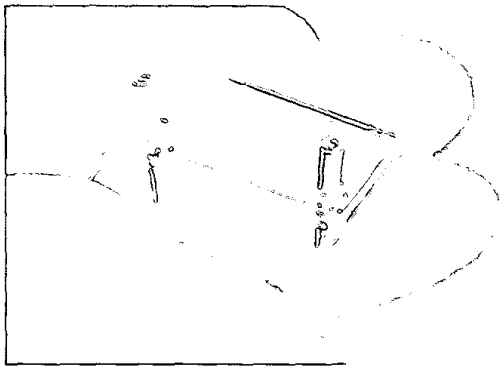

Figure 7: Lower view of the assembled LMTP.

5 LMTP evaluation

All characterisations of pump performance were performed by mass transfer of filtered DI water from a Sartorious 210s precision microbalance whose data was processed in real time by software written in Labview® (National Instruments) to obtain mass flow rate values.

To form a contiguous fluid circuit to the output reservoir on the balance, devices were primed via a Teflon tube which interconnected the pump and an input reservoir-bottle, pressurised to 20 kPa with Nitrogen, and filled with filtered, degassed, DI-water. Once primed, the input reservoir was vented to atmosphere and the pressure across the pump due to the height difference of the fluid in the reservoirs was zeroed by adjusting the height of the input reservoir with respect to the output reservoir to achieve zero mass transfer. Back pressures were applied during experimentation by means of precisely pneumatically pressurising the fluid container to which the pump transferred the fluid, using filtered compressed air and a subminiature pressure regulator (Type 91, Marsh Bellofram, UK).

As is the case with all micropumps, objective evaluation of performance required the external flow resistances of tubing in the associated measuring system to be measured and allowed for.

Evaluations were performed at voltages between ± 20 V and ± 180 V. Waveform generation was via a bespoke microcontroller system and 'H-bridge' drive electronics employing power-FETs. As we have reported [3], the possibility of bubble formation due to excessive rates of pressure change within the device is prevented by mildly restricting the drive waveform rise and fall times by using a simple series resistor to form a 200 μs time-constant with the piezoelectric actuators intrinsic capacitance. The microcontroller allows predetermined sequences of frequency steps to be applied in order to characterise frequency dependent characteristics.

6 Results

Figure 8 displays pumping rate as a function of driving frequency. Pumping rate can be seen to reduce in the region of 700 Hz. Whilst we have not investigated this in detail, we note that this coincides reasonably with a structural resonance of the overall MTP device that was previously identified in earlier designs by laser vibrometry [3] and it is considered possible that the new LMTP may be more susceptible to this resonant mode than were previous MTPs.

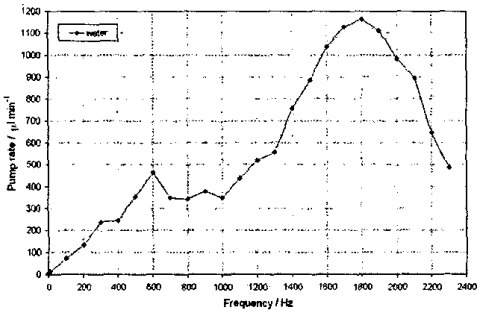

Figure 8: LMTP water pumping rate as a function of drive frequency.

Figure 9, shows the relationship between pumping rate as a function of back-pressure at the peak pumping frequency and drive level.

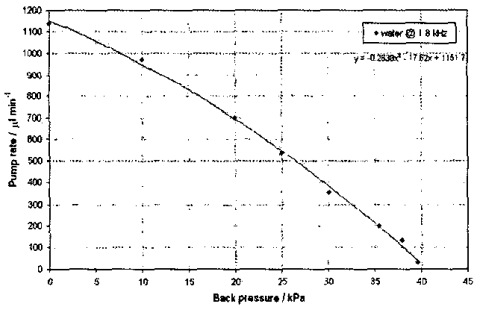

Figure 9: LMTP water pumping rate as a function of back-pressure at 1.8 kHz and ± 180 V drive amplitude.

Figure 10 displays pumping-rate as a function of drive voltage at the peak pumping frequency. This would be the operating condition under which an LMTP would be employed. Pumping performance would be controlled by either voltage modulation, or perhaps by pulse density modulation, in order to simplify high voltage drive circuitry at the cost of control logic.

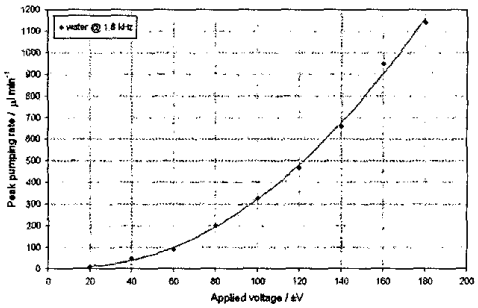

Figure 10: LMTP pumping rate as a function of drive voltage, at a drive frequency of 1.8 kHz.

In order to visualise the flow patterns occurring during operation of an LMTP and hence examine differences between its flow behaviour and that of a conventional circular MTP pump chamber, images were obtained whilst pumping a suspension of 5 µm diameter polystyrene microspheres (Duke Scientific Corp, CA, USA). The pumps were operated over frequency ranges up to their respective peak frequencies of 1.1 kHz for the circular MTP [4] and 1.8 kHz for the LMTP. Video images were obtained at 25 frames per second and therefore represent a composite, averaged, view of the flow within the pump rather than showing the trajectories of individual beads. Figure 11 demonstrates the flow patterns recorded within the circular chamber MTP. It can be seen that at the entrance to the pump chamber from the throttle there are regions of recirculation. These regions were relatively stable and were present to some extent over the majority of the pump's frequency range. However, they are not as accentuated as the recirculation patterns reported by Anderson et al [1] whose pump design incorporated more pronounced changes in physical dimensions.

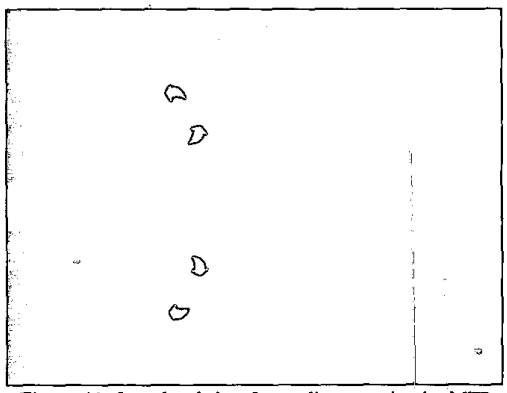

Figure 11: 5 µm beads in a 3 mm diameter circular MTP pumping at 1.1 kHz. The input throttle is to the left. Superimposed arrows highlight recirculation patterns.

Figure 12 shows the flow patterns present within the LMTP. It can be seen that there are no significant regions of

recirculation compared to those in the circular pump. This pattern was also stable over the frequency range of the pump.

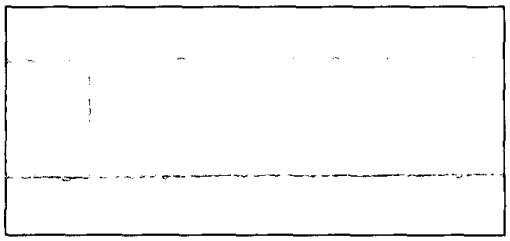

Figure 12: 5 μm diameter beads in a 1 mm wide channel LMPT pumping at 1.8 kHz. The input throttle is on the left.

7 Conclusions

We have further demonstrated that elastomeric substrates allow interesting forms of dynamic microstructures that circumvent some design restrictions imposed by rigid substrates upon the use of actuators.

The LMTP, by continuing to build upon this freedom, has further extended the performance of MTP-type micropumps: specifically by delivering fluid transport rates beyond one-millilitre per minute, whilst offering worthwhile back-pressures and, unusually, solid-phase suspension compatibility, within a compact, simple, straightforwardly fabricated structure.

We can crudely assign a figure of merit to such pumps by means of a *maximum pump-rate (ml)* × *maximum back-pressure (kPa)* product. This LMTP design yields a figure of merit of 44 whereas our previous circular chamber MTP design [4] yielded a figure of 19.

Whilst we have not sought to optimise the LMTP, recent modelling leads us to anticipate that still higher performance would result from revised placement of the microthrottles. It would also be desirable to investigate suppression of the suspected structural resonant mode at 700 Hz that manifests as a peak and dip in the frequency response and is highlighted by laser-vibrometric analysis.

Acknowledgements

We would like to thank Mr. Roger Traynor of Lambda Photometrics UK for his generous support and enthusiasm in performing the laser vibrometric measurements featured here.

References

[1] H. Andersson, W. van der Wijngarart, P. Nilsson, P Enoksson and G. A. Stemme. Valveless diffuser micropump for microfluidic analytical systems, Sensors and Actuators B, 72, pp. 259-265, (2001).

[2] I. D. Johnston, J. B. Davis, R. Richter, G. I. Herbert and M. C. Tracey. Elastomer-glass micropump employing active throttles, The Analyst, 129, pp. 829-34, (2004).

[3] I. D. Johnston, M. C. Tracey, J. B. Davis and C. K. L. Tan. Microfluidic solid phase suspension transport with an elastomer-based, single piezo-actuator, micro throttle pump, Lab Chip, 5, pp. 318-25, (2005).

[4] I. D. Johnston, M. C. Tracey, J. B. Davis and C. K. L. Tan. Micro throttle pump employing displacement amplification in an elastomeric substrate, J. Micromech. Microeng., 15, pp. 1831-1839, (2005).

[5] S. Shoji and M. Esashi. Microflow devices and systems, J. Micromech. Microeng, 4, pp. 157-171, (1994).

[6] P. Woias. Micropumps: summarizing the first two decades, Proc. SPIE 2001, 4560, pp. 39-52 (2001).